

1 TITLE:

2 **Stimulus-driven brain rhythms within the alpha band: The attentional-modulation conundrum**

3

4 ABBREVIATED TITLE: Reversed attentional modulation of alpha and SSRs

5

AUTHORS:	Affiliation	ORCID	Twitter
Christian Keitel*	1	0000-0003-2597-5499	@KeiCetel
Anne Keitel	1,2	0000-0003-4498-0146	@anneke_sci
Christopher SY Benwell	1,2	0000-0002-4157-4049	@ChrisSYBenwell
Christoph Daube	1	0000-0002-1763-8508	@christophdaube
Gregor Thut	1	0000-0003-1313-4262	
Joachim Gross	1,3	0000-0002-3994-1006	@Joachim__Gross

6

7 AFFILIATIONS:

8 **1** – Institute of Neuroscience and Psychology, University of Glasgow, 62 Hillhead Street, Glasgow
9 G12 8QB, UK; **2** – Psychology, School of Social Sciences, University of Dundee, Scrymgeour Building,
10 Dundee DD1 4HN, UK; **3** – Institut für Biomagnetismus und Biosignalanalyse, Westfälische Wilhelms-
11 Universität, Malmedyweg 15, 48149 Münster, Germany

12 * – corresponding author, christian.keitel@glasgow.ac.uk

13

14 KEYWORDS: alpha rhythm, entrainment, phase synchronisation, spatial attention, steady-state
15 response (SSR), frequency tagging

16

17 ACKNOWLEDGMENTS: Funded by a Wellcome Trust Joint Investigator Grant awarded to GT and JG
18 (#098433/#098434). Lucy Dewhurst and Jennifer McAllister assisted in data collection. The
19 experimental stimulation was realized using Cogent Graphics developed by John Romaya at the
20 Laboratory of Neurobiology, Wellcome Department of Imaging Neuroscience, University College
21 London (UCL).

22

0 Table(s), 6 Figure(s), 0 Footnote(s)

23 **ABSTRACT**

24 Two largely independent research lines use rhythmic sensory stimulation to study visual processing.
25 Despite the use of strikingly similar experimental paradigms, they differ crucially in their notion of
26 the stimulus-driven periodic brain responses: One regards them mostly as synchronised (entrained)
27 intrinsic brain rhythms; the other assumes they are predominantly evoked responses (classically
28 termed steady-state responses, or SSRs) that add to the ongoing brain activity. This conceptual
29 difference can produce contradictory predictions about, and interpretations of, experimental
30 outcomes. The effect of spatial attention on brain rhythms in the alpha-band (8 – 13 Hz) is one such
31 instance: alpha-range SSRs have typically been found to *increase* in power when participants focus
32 their spatial attention on laterally presented stimuli, in line with a gain control of the visual evoked
33 response. In nearly identical experiments, retinotopic *decreases* in entrained alpha-band power have
34 been reported, in line with the inhibitory function of intrinsic alpha. Here we reconcile these
35 contradictory findings by showing that they result from a small but far-reaching difference between
36 two common approaches to EEG spectral decomposition. In a new analysis of previously published
37 human EEG data, recorded during bilateral rhythmic visual stimulation, we find the typical SSR gain
38 effect when emphasising stimulus-locked neural activity and the typical retinotopic alpha
39 suppression when focusing on ongoing rhythms. These opposite but parallel effects suggest that
40 spatial attention may bias the neural processing of dynamic visual stimulation via two
41 complementary neural mechanisms.

42 **SIGNIFICANCE STATEMENT**

43 Attending to a visual stimulus strengthens its representation in visual cortex and leads to a
44 retinotopic suppression of spontaneous alpha rhythms. To further investigate this process,
45 researchers often attempt to phase-lock, or entrain, alpha through rhythmic visual stimulation under
46 the assumption that this entrained alpha retains the characteristics of spontaneous alpha. Instead,
47 we show that the part of the brain response that is phase-locked to the visual stimulation *increased*
48 with attention (in line with steady-state evoked potentials), while the typical suppression was only
49 present in non-stimulus-locked alpha activity. The opposite signs of these effects suggest that
50 attentional modulation of dynamic visual stimulation relies on two parallel cortical mechanisms –
51 retinotopic alpha suppression and increased temporal tracking.

52

53 INTRODUCTION

54 Cortical visual processing has long been studied using rhythmic sensory stimulation (Adrian and
55 Matthews, 1934; Walter et al., 1946; Regan, 1966). This type of stimulation drives continuous brain
56 responses termed steady-state responses (SSRs) that reflect the temporal periodicities in the
57 stimulation precisely. SSRs allow tracking of individual stimuli in multi-element displays (Vialatte et
58 al., 2010; Norcia et al., 2015). Further, they readily indicate cognitive biases of cortical visual
59 processing, such as the selective allocation of attention (Morgan et al., 1996; Keitel et al., 2013;
60 Stormer et al., 2014).

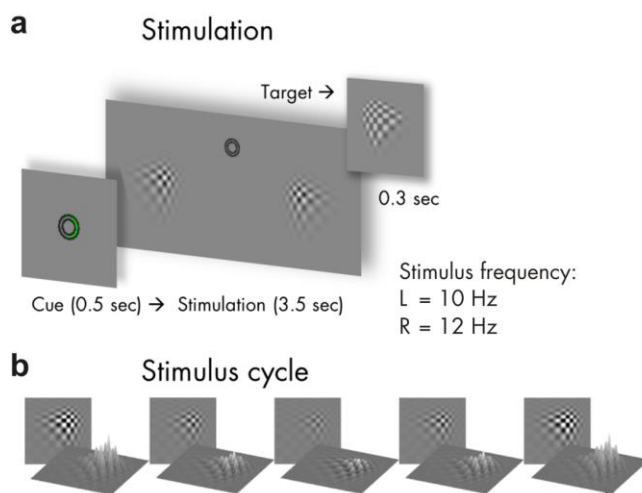
61 Although SSRs can be driven using a wide range of frequencies (Herrmann, 2001), stimulation at
62 alpha band frequencies (8 – 13 Hz) has stirred particular interest. Alpha rhythms dominate brain
63 activity in occipital visual cortices (Groppe et al., 2013; Keitel and Gross, 2016) and influence
64 perception (Benwell et al., 2017; Iemi et al., 2017; Samaha et al., 2017; Benwell et al., 2018).
65 Researchers have therefore used alpha-rhythmic visual stimulation in attempts to align the phase of
66 – or *entrain* – intrinsic alpha rhythms and consequently provided evidence for visual alpha
67 entrainment (Mathewson et al., 2012; Zauner et al., 2012; Spaak et al., 2014; Gulbinaite et al., 2017).
68 These findings suggest that at least part of the SSR driven by alpha-band stimulation should be
69 attributed to entrained alpha generators (Notbohm et al., 2016).

70 Some issues remain with such an account (Capilla et al., 2011; Keitel et al., 2014). For instance,
71 experiments have consistently reported SSR power increases when probing effects of spatial
72 selective attention on SSRs driven by lateralised hemifield stimuli (Müller et al., 1998a), also when
73 using alpha-band frequencies (Kim et al., 2007; Kashiwase et al., 2012; Keitel et al., 2013). However,
74 recent studies that used similar paradigms, but treated alpha-frequency SSRs as phase-entrained
75 alpha rhythms in line with an earlier study using rhythmic transcranial magnetic stimulation (Herring
76 et al., 2015), reported the opposite effect (Kizuk and Mathewson, 2017; Gulbinaite et al., 2019).
77 Oscillatory brain activity showed attentional modulations characteristic of the intrinsic alpha rhythm
78 during stimulation: Alpha power decreased over the hemisphere contralateral to the attended
79 position, an effect known to be part of a retinotopic alpha power lateralisation during selective
80 spatial attention (Worden et al., 2000; Kelly et al., 2006; Thut et al., 2006; Rihs et al., 2007; Capilla et
81 al., 2012). Briefly put, studies analysing SSRs show a power *increase*, whereas studies analysing
82 “entrained alpha” show a power *decrease* with attention.

83 Both neural responses originate from visual cortices contralateral to the hemifield position of the
84 driving stimuli (Keitel et al., 2013; Spaak et al., 2014). Assuming a single underlying neural process,
85 opposite attention effects therefore seemingly contradict each other. However, results in support of

86 alpha entrainment differed in how exactly responses to the periodic stimulation were quantified.
87 Effects consistent with SSR modulation resulted from spectral decompositions performed on trial-
88 averaged EEG waveforms. This approach tunes the resulting power estimate to the part of the neural
89 response that is sufficiently time-locked to the stimulation (Tallon-Baudry et al., 1996; Delorme and
90 Makeig, 2004). Effects consistent with alpha entrainment instead typically result from averages of
91 single-trial spectral transforms, thus emphasising intrinsic non-phase-locked activity (Tallon-Baudry
92 et al., 1998; Herrmann et al., 2004). Both approaches have been applied before to compare stimulus-
93 evoked and induced brain rhythms in alpha (Moratti et al., 2007) and gamma frequency ranges
94 (~40 Hz; Tallon-Baudry et al., 1998; Picton et al., 2003). Here we focussed on contrasting the
95 attentional modulation of alpha during- and SSRs driven by an alpha-rhythmic stimulation.

96 We therefore compared the outcome of both approaches in a new analysis of previously reported
97 EEG data (Keitel et al., 2017b). Participants viewed two lateralised stimuli, both flickering at alpha
98 band frequencies (10 and 12 Hz). They were cued to focus on one of the two and perform a target
99 detection task at the attended position. We quantified spectral power estimates according to both
100 approaches described above from the same EEG data. Should the outcome depend on the approach
101 taken, we expected to find the typical alpha power lateralisation (contralateral < ipsilateral) when
102 averaging single-trial power spectra. In power spectra of trial-averaged EEG instead we expected the
103 typical SSR power gain modulation in the opposite direction (contralateral > ipsilateral). Crucially,
104 such an outcome would warrant a re-evaluation of stimulus-driven brain rhythms in the alpha range
105 and intrinsic alpha as a unitary phenomenon (alpha entrainment).



106

107

108 **Figure 1** Stimulus schematics and trial time course. (a) shows the time course of one trial with a cue
109 displayed for 0.5 sec (here: Attend Right), followed by the bilateral visual stimulation for 3.5 sec. Left
110 (L) stimulus contrast fluctuated with a rate of 10 Hz and Right (R) stimulus contrast at 12 Hz. Targets
111 that participants were instructed to respond to were slightly altered versions of the stimuli (see

112 inset) that were displayed occasionally for 0.3 sec. **(b)** Rhythmic visual stimulation was achieved by a
113 frame-by-frame adjustment of global stimulus contrast (through local luminance changes) as
114 exemplified here in one representative cycle.
115

116 **METHODS**

117 **Participants**

118 For the present report, we re-analysed EEG data of 17 volunteers recorded in an earlier study (Keitel
119 et al., 2017a). Participants (13 women; median age = 22 yrs, range = 19 – 32 yrs) declared normal or
120 corrected-to-normal vision and no history of neurological diseases or injury. All procedures were
121 approved by the ethics committee of the College of Science & Engineering at the University of
122 Glasgow (application no. 300140020) and adhered to the guidelines for the treatment of human
123 subjects in the Declaration of Helsinki. Volunteers received monetary compensation of £6/h. They
124 gave informed written consent before participating in the experiment. Note that we excluded five
125 additional datasets on grounds reported in the original study (four showed excessive eye
126 movements, one underperformed in the task).

127 **Stimulation**

128 Participants viewed experimental stimuli on a computer screen (refresh rate = 100 frames per sec) at
129 a distance of 0.8 m that displayed a grey background (luminance = 6.5 cd/m²). Small concentric
130 circles in the centre of the screen served as a fixation point (*Figure 1*). Two blurry checkerboard
131 patches (horizontal/vertical diameter = 4° of visual angle) were positioned at an eccentricity of 4.4°
132 from central fixation, one each in the lower left and lower right visual quadrants. Both patches
133 changed contrast rhythmically during trials: Stimulus contrast against the background was modulated
134 by varying patch peak luminance between 7.5 cd/m² (minimum) and 29.1 cd/m² (maximum).

135 On each screen refresh, peak luminance changed incrementally to approach temporally smooth
136 contrast modulations as opposed to a simple on-off flicker (Andersen and Muller, 2015). Further
137 details of the stimulation can be found in Keitel et al. (2017a). The contrast modulation followed a
138 10-Hz periodicity for the left and a 12-Hz periodicity for the right stimulus. Note that the experiment
139 featured further conditions displaying quasi-rhythmic contrast modulations in different frequency
140 bands. Corresponding results can be found in the original report and will not be considered in the
141 present analysis.

142 **Procedure and Task**

143 Participants performed the experiment in an acoustically dampened and electromagnetically
144 shielded chamber. In total, they were presented with 576 experimental trials, subdivided into 8

145 blocks with durations of ~5 min each. Between blocks, participants took self-paced breaks. Prior to
146 the experiment, participants practiced the behavioural task (see below) for at least one block. After
147 each block they received feedback regarding their accuracy and response speed. The experiment was
148 comprised of 8 conditions (= 72 trials each) resulting from a manipulation of the two factors
149 attended position (left vs. right patch) and stimulation frequency (one rhythmic and three quasi-
150 rhythmic conditions) in a fully balanced design. Trials of different conditions were presented in
151 pseudo-random order. As stated above, the present study focussed on the two conditions featuring
152 fully rhythmic stimuli. Corresponding trials ($N = 144$) were thus selected a posteriori from the full
153 design.

154 Single trials began with cueing participants to attend to the left or right stimulus for 0.5 sec, followed
155 by presentation of the dynamically contrast-modulating patches for 3.5 sec (*Figure 1*). After patch
156 offset, an idle period of 0.7 sec allowed participants to blink before the next trial started.

157 To control whether participants maintained a focus of spatial attention, they were instructed to
158 respond to occasional brief “flashes” (0.3 sec) of the cued stimulus (= targets) while ignoring similar
159 events in the other stimulus (= distracters). Targets and distracters occurred in one third of all trials
160 and up to 2 times in one trial with a minimum interval of 0.8 sec between subsequent onsets.

161 Detection was reported as speeded responses to flashes (recorded as space bar presses on a
162 standard keyboard).

163 **Behavioural data recording and analyses**

164 Flash detections were considered a ‘hit’ when a response occurred from 0.2 to 1 sec after target
165 onset. Delays between target onsets and responses were considered reaction times (RT). Statistical
166 comparisons of mean accuracies (proportion of correct responses to the total number of targets and
167 distracters) and median RTs between experimental conditions were conducted and reported in
168 (2017a). In the present study, we did not consider the behavioural data further. Note that the
169 original statistical analysis found that task performance in Attend-Left and Attend-Right conditions
170 was comparable.

171 **Electrophysiological data recording**

172 EEG was recorded from 128 scalp electrodes and digitally sampled at a rate of 512 Hz using a BioSemi
173 ActiveTwo system (BioSemi, Amsterdam, Netherlands). Scalp electrodes were mounted in an elastic
174 cap and positioned according to an extended 10-20-system (Oostenveld and Praamstra, 2001).

175 Lateral eye movements were monitored with a bipolar outer canthus montage (horizontal electro-

176 oculogram). Vertical eye movements and blinks were monitored with a bipolar montage of
177 electrodes positioned below and above the right eye (vertical electro-oculogram).

178 **Electrophysiological data pre-processing**

179 From continuous data, we extracted epochs of 5 s, starting 1 s before patch onset using the MATLAB
180 toolbox EEGLAB (Delorme and Makeig, 2004). In further pre-processing, we excluded epochs that
181 corresponded to trials containing transient targets and distracters (24 per condition) as well as
182 epochs with horizontal and vertical eye movements exceeding 20 μV ($\sim 2^\circ$ of visual angle) or
183 containing blinks. For treating additional artefacts, such as single noisy electrodes, we applied the
184 ‘fully automated statistical thresholding for EEG artefact rejection’ (FASTER; Nolan et al., 2010). This
185 procedure corrected or discarded epochs with residual artefacts based on statistical parameters of
186 the data. Artefact correction employed a spherical-spline-based channel interpolation. Epochs with
187 more than 12 artefact-contaminated electrodes were excluded from analysis.

188 From 48 available epochs per condition, we discarded a median of 14 epochs for the Attend-Left
189 conditions and 15 epochs for the Attend-Right conditions per participant with a between-subject
190 range of 6 to 28 (Attend-Left) and 8 to 31 epochs (Attend-Right). Within-subject variation of number
191 of epochs per condition remained small with a median difference of 3 trials (maximum difference = 9
192 for one participant).

193 Subsequent analyses were carried out in Fieldtrip (Oostenveld et al., 2011) in combination with
194 custom-written routines. We extracted segments of 3 s starting 0.5 s after patch onset from pre-
195 processed artefact-free epochs (5 s). Data prior to stimulation onset (1 s), only serving to identify eye
196 movements shortly before and during cue presentation, were omitted. To attenuate the influence of
197 stimulus-onset evoked activity on EEG spectral decomposition, the initial 0.5 s of stimulation were
198 excluded. Lastly, because stimulation ceased after 3.5 s, we also discarded the final 0.5 s of original
199 epochs.

200 **Electrophysiological data analyses – spectral decomposition**

201 Artefact-free 3-sec epochs were converted to scalp current densities (SCDs), a reference-free
202 measure of brain electrical activity (Ferree, 2006; Kayser and Tenke, 2015), by means of the spherical
203 spline method (Perrin et al., 1987) as implemented in Fieldtrip (function *ft_scalpcurrentdensity*,
204 method ‘spline’, $\lambda = 10^{-4}$). Detrended (i.e. mean and linear trend removed) SCD time series
205 were then Tukey-tapered and subjected to Fourier transforms while employing zero-padding in order
206 to achieve a frequency-resolution of 0.25 Hz. Crucially, from resulting complex Fourier spectra we
207 calculated two sets of aggregate power spectra with slightly different approaches. First, we

208 calculated power spectra as the average of squared absolute values of complex Fourier spectra (Z) as
209 follows:

$$210 \quad onPOW(f) = \frac{1}{n} \sum_{i=1}^n |Z_i(f)|^2 \quad [1]$$

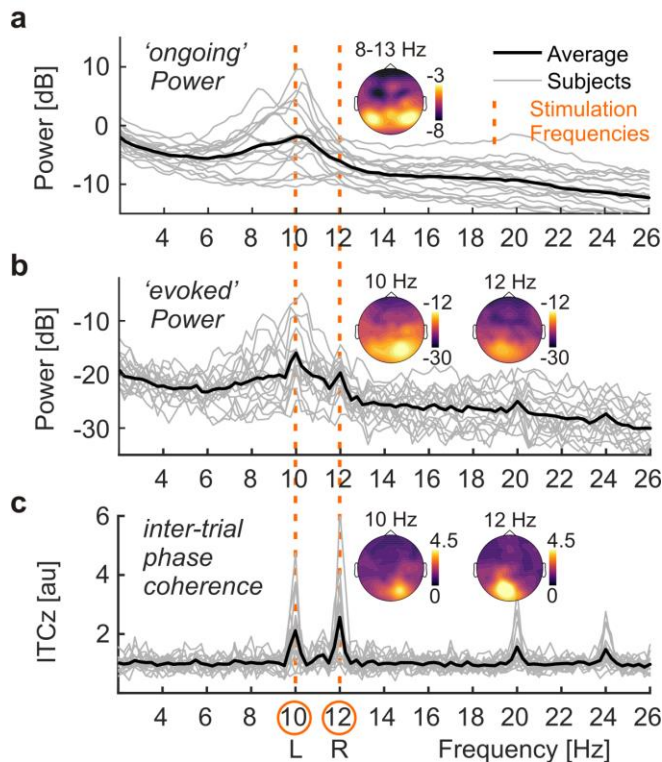
211 where *onPOW* is the classical power estimate for ongoing (intrinsic) oscillatory activity for frequency
212 f and n is the number of trials. Secondly, we additionally calculated the squared absolute value of the
213 averaged complex Fourier spectra according to:

$$214 \quad evoPOW(f) = \left| \frac{1}{n} \sum_{i=1}^n Z_i(f) \right|^2 \quad [2]$$

215 The formula yields *evoPOW*, or evoked power, an estimate that is identical with the frequency-
216 tagging standard approach of averaging per-trial EEG time series before spectral decomposition. This
217 step is usually performed to retain only the truly phase-locked response to the stimulus (Tallon-
218 Baudry et al., 1996). Note that both formulas only differ in the order in which weighted sums and
219 absolute values are computed. Also note that formula [2] is highly similar to the calculation of inter-
220 trial phase coherence (ITC), a popular measure of phase locking (Cohen, 2014; Gross, 2014; van
221 Diepen and Mazaheri, 2018). ITC calculation additionally includes a trial-by-trial amplitude
222 normalisation. To complement our analysis we thus quantified ITC according to:

$$223 \quad ITC(f) = \left| \frac{1}{n} \sum_{i=1}^n \frac{Z_i(f)}{|Z_i(f)|} \right| \quad [3]$$

224 For further analyses, power spectra were normalised by converting them to decibel scale, i.e. taking
225 the decadic logarithm, then multiplying by 10 (hereafter termed log power spectra). ITC was
226 converted to ITCz to reduce the bias introduced by differences in trial numbers between conditions
227 (Bonfond and Jensen, 2012; Samaha et al., 2015).



228
229

230 **Figure 2** EEG spectral decomposition. (a) Power spectra collapsed across conditions and all electrode
231 positions below the sagittal midline for single subjects (light grey lines) and group averages (strong
232 black line). Note the characteristic alpha peaks in the frequency range of 8 – 13 Hz. Inset scalp map
233 shows topographical distribution of alpha power on a dB scale based on scalp current densities. (b)
234 Same as in (a) but for ‘evoked’ power. Distinct peaks are visible at stimulation frequencies 10 & 12 Hz
235 (dashed vertical orange lines across plots). Inset scalp maps show topographical distributions of SSR
236 power at 10 & 12 on a dB scale. Note the difference in scale between ongoing power in (a) and
237 evoked power (b). (c) Same as in (a) but for inter-trial phase-locking (ITCz). Inset scalp maps show
238 topographical distributions of SSR ITCz at 10 & 12.

239

240 **Alpha power – attentional modulation and lateralisation**

241 Spectra of ongoing power (*onPOW*), pooled over both experimental conditions and all electrodes,
242 showed a prominent peak in the alpha frequency range (*Figure 2*). We used mean log ongoing power
243 across the range of 8 – 13 Hz to assess intrinsic alpha power modulations by attention. Analysing
244 Attend-Right and Attend-Left conditions separately, yielded two alpha power topographies for each
245 participant. These were compared by means of cluster-based permutation statistics (Maris and
246 Oostenveld, 2007) using $N = 5000$ random permutations. We clustered data across channel
247 neighbourhoods with an average size of 7.9 channels that were determined by triangulated sensor
248 proximity (function *ft_prepare_neighbours*, method ‘triangulation’). The resulting probabilities (P -
249 values) were corrected for two-sided testing. Subtracting left-lateralised (Attend-Left conditions)
250 from right-lateralised (Attend-Right) alpha power topographies, we found a right-hemispheric

251 positive and a left-hemispheric negative cluster of electrodes that was due to the retinotopic effects
252 of spatial attention on alpha power lateralisation (*Figure 3*), similar to an earlier re-analysis of the
253 other conditions of this experiment (Keitel et al., 2018).

254 Finally, we tested the difference between Attend-Left and Attend-Right conditions, i.e. attention
255 effects for left- and right-hemispheric clusters separately. To this end, we submitted alpha power
256 differences (contralateral hemifield attended minus ignored) to Bayesian one-sample t-tests against
257 zero (Rouder et al., 2009). Attention effects were further compared against each other by means of a
258 Bayesian paired-samples t-test as implemented in JASP (JASP-Team, 2018) with a Cauchy prior scaled
259 to $r = 0.5$, putting more emphasis on smaller effects (Rouder et al., 2012; Schonbrodt and
260 Wagenmakers, 2017).

261 This procedure allowed us to quantify the evidence in favour of the null vs the alternative hypothesis
262 (H_0 vs H_1). For each test, the corresponding Bayes factor (called BF_{10}) showed evidence for H_1
263 (compared to H_0) if it exceeded a value of 3, and no evidence for H_1 if $BF_{10} < 1$, with the intervening
264 range 1 – 3 termed ‘anecdotal evidence’ by convention (Wagenmakers et al., 2011). Inverting BF_{10} , to
265 yield a quantity termed BF_{01} , served to quantify evidence in favour of H_0 on the same scale. For BF_{10}
266 and BF_{01} , values < 1 were taken as inconclusive evidence for either hypothesis. Note that for the sake
267 of brevity we report errors in BF estimates only when exceeding 0.001%.

268 **SSR power – attentional modulation**

269 Spectra of evoked power, pooled over both experimental conditions and all electrodes, revealed
270 periodic responses to the two stimuli at the respective stimulation frequencies, 10 and 12 Hz
271 (*Figure 2*). Therefore, we assessed attention effects for these two spectral SSR representations. Two
272 separate cluster-based permutation tests, one for each stimulation frequency, contrasted evoked
273 power topographies between attended and ignored (= other stimulus attended) conditions. Two-
274 sided tests were performed with the same parameters as for alpha power (see above).

275 Again, we found one electrode cluster carrying systematic attention effects per frequency. As for
276 alpha, SSR power from these two clusters were subjected to separate Bayesian one-sample t-tests
277 against zero (one-sided, attended $>$ ignored) and compared against each other by means of a
278 Bayesian paired-sample t-test (two-sided).

279 **SSR inter-trial phase coherence – attentional modulation**

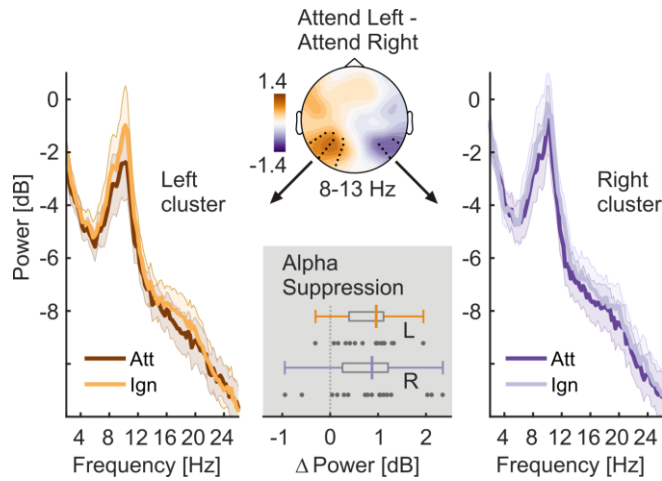
280 We also evaluated a pure measure of neural phase-locking to the stimulation, SSR inter-trial phase
281 coherence (ITC), because evoked power can be regarded as a hybrid measure depending on both the
282 amplitude of the underlying rhythmic response and the consistency of its phase across trials. ITC

283 indicates only the latter as SSRs are set to unit amplitude prior to summing across trials (see
284 formula 3). ITC spectra, pooled over both experimental conditions and all electrodes, showed distinct
285 neural phase-locking at the respective driving frequencies, 10 and 12 Hz (*Figure 2*). Cluster-based
286 permutation testing confirmed topographic regions that showed systemic gain effects in ITC.
287 Subsequently, the same Bayesian inference was applied to data from these clusters as for SSR power.

288 **Correlation of alpha and SSR attention effects – group level**

289 As a consequence of our counter-intuitive finding that SSR attention effects appeared strongest over
290 occipital regions ipsi-lateral to the driving stimulus (see Results section *SSR power & inter-trial phase*
291 *locking – attentional modulation* below), we explored a posteriori whether these effects could be
292 explained by ipsilateral increases in alpha power during focussed attention. We correlated attention
293 effects on alpha and SSR power using Bayesian inference (rank correlation coefficient Kendall's tau-b
294 or τ_b , beta-prior = 0.75) to test for a positive linear relationship. More specifically, we correlated the
295 left-hemispheric alpha power suppression (Ignored minus Attended) with the 10-Hz SSR (evoked)
296 power attention effect (Attended minus Ignored) and the right-hemispheric alpha power suppression
297 with the 12-Hz SSR power attention effect. We opted for these combinations because the
298 corresponding effects overlapped topographically (see Results). Along with the correlation coefficient
299 ρ , we report its 95%-Credible Interval (95%-CrI).

300 We also probed the linear relationship between alpha power and SSR ITC attention effects. Because
301 ITC gains were not clearly lateralised, we collapsed gain effects (Attended minus Ignored) across both
302 stimulation frequencies and correlated these with a hemisphere-collapsed alpha suppression index.
303 This index was quantified as the halved sum of left and right-hemispheric suppression effects as
304 retrieved from significant clusters in the topographical analysis of alpha power differences (Attend
305 Left minus Attend Right), shown in *Figure 3*. Again, we expected a positive correlation here if alpha
306 power suppression influenced phase-locking to visual stimulation. For means of comparison, we
307 repeated this analysis with attention effects on SSR power collapsed across frequencies.



308

309 **Figure 3** Allocation of spatial attention produces retinotopic alpha power modulation. The scalp map
310 (top, center) depicts alpha power lateralisation (Attend Left – Attend right conditions) on a dB scale.
311 Black dots indicate left- and right-hemispheric electrode-clusters that showed a consistent difference
312 in group statistics (two-tailed cluster-based permutation tests). Left and right spectra illustrate alpha
313 power differences in respective clusters when the contralateral hemifield was attended (Att) versus
314 ignored (Ign). The bottom grey inset depicts the distribution of individual alpha power suppression
315 effects (Ignored minus Attended) within left (L) and right (R) hemisphere clusters in the 8 – 13 Hz
316 band. Boxplots indicate interquartile ranges (boxes) and medians (coloured vertical intersectors).
317 Dots below show individual effects (1 dot = 1 participant).

318 **Alpha and SSR attention effects – subject level regression**

319 The relationship between alpha power (lateralisation) and SSR attentional modulation was further
320 subjected to a more fine-grained analysis considering within-subject variability across single trials
321 and allowing for a better control of between-subject differences in alpha and SSR power. We
322 assumed that if the SSR attention effect (i.e. the ipsilateral SSR power gain) was a mere consequence
323 of the co-localised alpha power increase then these two effects should co-vary across trials. For this
324 analysis we recalculated single-trial alpha power and SSR evoked power / ITC estimates at each EEG
325 sensor and for both conditions in each subject based on the same artefact-removed EEG epochs and
326 using the same spectral decomposition as described above. Because ITC is not defined for single
327 trials, we used a Jackknife approach that computed single trial estimates in a leave-one-out
328 procedure and allowed for subsequent evaluation of inter-trial variability (Richter et al., 2015). For
329 consistency, we computed similar alpha-power Jackknife estimates. From these estimates, we
330 calculated attention effects as all possible pairwise differences between trials of different conditions
331 (Attend Left vs Attend Right), yielding distributions of alpha power hemispheric lateralisation and SSR
332 evoked power / ITC attentional modulation (for 10 & 12 Hz SSRs separately). To validate this
333 approach, we used it to reproduce alpha power and SSR attention effects described below (data not
334 shown, reproducible via code in online repository (Keitel et al., 2017b)).

335 We then tested for a linear relationship between both z-scored measures by subjecting them to a
336 robust linear regression (MATLAB function 'robustfit', default options), carried out for each EEG
337 sensor separately. The obtained subject-specific regression coefficients β (slopes) were entered into
338 a group statistical test. We tested slopes against zero (i.e. no linear relationship) by means of cluster-
339 based permutation tests (two-tailed), clustering across EEG sensors. Four tests were carried out in
340 total; one for each regression of alpha power lateralisation with SSR evoked power or SSR ITC
341 attentional modulation, and separately for 10 & 12 Hz SSR, respectively. This procedure was
342 supplemented by sensor-by-sensor Bayesian t-tests (Rouder et al., 2009) to quantify the evidence in
343 favour of a linear vs no relationship (see Methods section *Alpha power – attentional modulation and*
344 *lateralisation* regarding Bayesian inference).

345

346 **RESULTS**

347 **Ongoing alpha power – attentional modulation and lateralisation**

348 The power of the ongoing alpha rhythm lateralised with the allocation of spatial attention to left and
349 right stimuli. A topographic map of the differences in alpha power between Attend-Left and Attend-

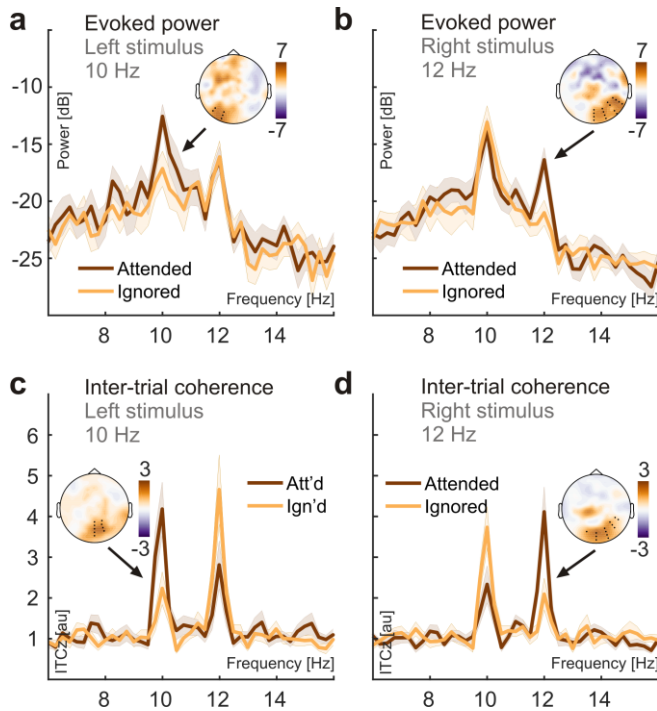
350 Right conditions shows significant left- and right-hemispheric electrode clusters (*Figure 3*). These
351 clusters signify retinotopic alpha power modulation when participants attended to left vs right
352 stimulus positions (right cluster: $t_{\text{sum}} = -21.454$, $P = 0.026$; left cluster: $t_{\text{sum}} = 81.264$, $P = 0.002$). The
353 differences are further illustrated in power spectra pooled over electrodes of each cluster (*Figure 3*).
354 As predicted, alpha power at each cluster was lower when participants attended to the contralateral
355 stimulus. Bayesian inference confirmed the alpha power attention effect for the right ($M = 0.806$ dB,
356 $SEM = 0.216$; $BF_{10} = 21.17$) and left cluster ($M = 0.790$ dB, $SEM = 0.133$; $BF_{10} = 906.36$). Both effects
357 were of comparable magnitude ($BF_{01} = 4.009 \pm 0.007$).

358 **SSR power & inter-trial phase locking – attentional modulation**

359 Crucially, we found the opposite pattern when looking at SSRs, i.e. the exact same data but with a
360 slightly different focus on oscillatory brain activity that was time-locked to the stimulation (compare
361 formulas 1 and 2): SSRs showed increased power when the respective driving stimulus was attended
362 versus ignored (*Figure 4*). The power of neural responses evoked by our stimuli (SSRs) was at least
363 one order of magnitude smaller than ongoing alpha power on average (difference > 10dB, i.e.
364 between 10 – 100 times). Nevertheless, SSRs could be clearly identified as distinct peaks in (evoked)
365 power and ITC spectra. Consistent with the retinotopic projection to early visual cortices,
366 topographical distributions of both measures showed a focal maxima contra-lateral to the respective
367 stimulus positions that were attended (*Figure 2*). Counter-intuitively though, maximum attention
368 effects on SSR power did not coincide topographically with sites that showed maximum SSR power
369 overall (compare scalp maps in *Figure 2 & 4*). Also, due to their rather ipsilateral scalp distributions
370 (with respect to the attended location), SSR attention effects did not match topographies of
371 attention-related decreases in ongoing alpha power (compare scalp maps in *Figures 3 & 4*). The 10-
372 Hz SSR driven by the left-hemifield stimulus showed a left-hemispheric power increase when
373 attended ($t_{\text{sum}} = 15.837$, $P = 0.059$). Similarly, attention increased the power of the 12-Hz SSR driven
374 by the right-hemifield stimulus in a right-hemispheric cluster ($t_{\text{sum}} = 53.282$, $P < 0.001$). Bayesian
375 inference confirmed the attention effect on 10-Hz ($M = 3.727$ dB, $SEM = 0.919$; $BF_{10} = 37.05$) and 12-
376 Hz SSR power ($M = 4.473$ dB, $SEM = 0.841$; $BF_{10} = 329.75$) averaged within clusters. Both effects were
377 of comparable magnitude ($BF_{01} = 3.443 \pm 0.005$).

378 SSR phase-locking (quantified as ITCz) also increased with attention to the respective stimulus. In
379 contrast to evoked power, topographical representations of these effects showed greater overlap
380 with the sites that showed maximum phase-locking in general (*Figure 4*). For both frequencies, ITCz
381 increased in central occipital clusters (10 Hz: $t_{\text{sum}} = 41.351$, $P = 0.004$; 12 Hz: $t_{\text{sum}} = 31.116$, $P = 0.012$).
382 Again, Bayesian inference confirmed the attention effect on 10-Hz ($M = 1.386$ au, $SEM = 0.297$;

383 $BF_{10} = 105.71$, one-sided) and 12-Hz ITCz ($M = 1.824$ au, $SEM = 0.451$; $BF_{10} = 36.11$, one-sided).
384 Evidence for a greater attention effect on 12-Hz than on 10-Hz ITC remained inconclusive
385 ($BF_{10} = 0.473$).



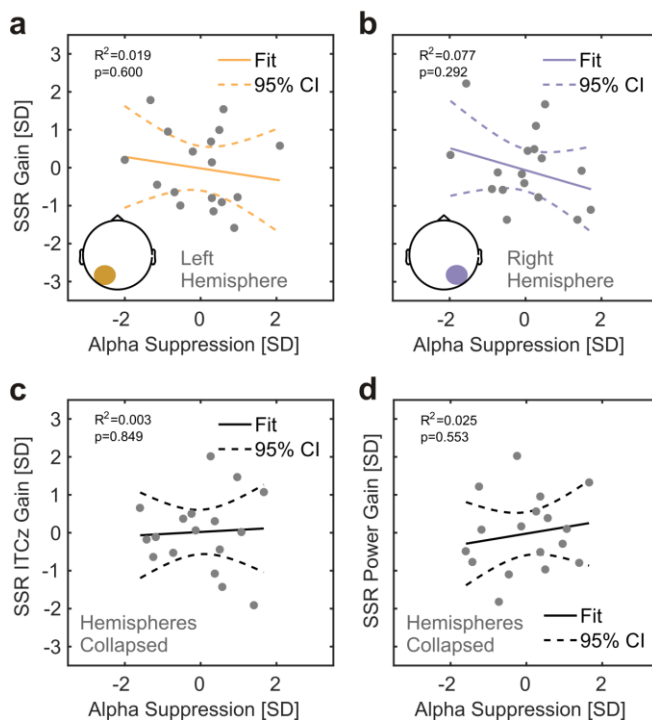
386

387 **Figure 4** Attention effects on SSR evoked power (evoPow) and SSR inter-trial phase coherence. (a)
388 SSR evoked power spectra show systematic power differences at the presentation frequency (10 Hz)
389 of the left stimulus when it was attended (dark red) versus ignored (orange). The inset scalp map
390 illustrates the topographical distribution of the attention effects. Power spectra were averaged
391 across electrodes (black dots in scalp maps) that showed consistent attention effects in group
392 statistics (two-tailed cluster-based permutation tests) for Attended and Ignored conditions
393 separately. (b) Same as in (a) but for the 12-Hz stimulus presented in the right visual hemifield. (c,d)
394 Same as in (a,b) but using ITCz as a measure of SSR inter-trial phase coherence.
395

396 Correlation of alpha and SSR attention effects – group level

397 Lastly, we tested whether the SSR attention gain effects were mere reflections of the topographically
398 coinciding ipsilateral ongoing alpha power increase during focussed attention that co-occurred with
399 the contralateral ongoing alpha-power decrease (Figure 3). Speaking against this account, Bayesian
400 inference provided moderate evidence against the expected positive correlations between the left-
401 hemispheric alpha attention effect and the 10-Hz SSR attention effect ($\tau_b = -0.221$, 95%-CrI = [0.002
402 0.269]; $BF_{01} = 5.811$) and between the right-hemispheric alpha attention effect and the 12-Hz SSR
403 attention effect ($\tau_b = -0.088$, 95%-CrI = [0.004 0.315]; $BF_{01} = 3.904$). These relationships are further
404 illustrated by corresponding linear fits in Figure 5.

405 Following this analysis, we further explored the relationship between spatially non-overlapping
 406 decreases in alpha-power contralateral to the attended position and the ipsilateral SSR power gain
 407 effects. For the lack of a specific hypothesis about the sign of the correlation in this case, we
 408 quantified the evidence for any relationship (two-sided test). The results remained inconclusive for a
 409 correlation between the left-hemispheric alpha attention effect and the right-hemispheric 12-Hz SSR
 410 attention effect ($\tau_b = 0.235$, 95%-CrI = [-0.110 0.487]; $BF_{01} = 1.280$) and between the right-
 411 hemispheric alpha attention effect and the left-hemispheric 10-Hz SSR attention effect ($\tau_b = 0.103$,
 412 95%-CrI = [-0.218 0.383]; $BF_{01} = 2.400$).



413
 414 **Figure 5** Relationships between attention effects on alpha power and SSRs. (a) Individual 10-Hz (left
 415 stimulus) SSR evoked power gain (Attended minus Ignored; z-scored, y-axis) as a function of alpha
 416 suppression (Ignored minus Attended; z-scored, x axis) in overlapping left-hemispheric parieto-
 417 occipital electrode clusters. Grey dots represent participants. Coloured lines depict a straight line fit
 418 and its confidence interval (dashed lines). Goodness of fit of the linear model provided as R^2 along
 419 with corresponding P-Value. As confirmed by additional tests, both attention effects do not show a
 420 positive linear relationship that would be expected if the ipsilateral SSR power gain effect was a
 421 consequence of the ipsilateral alpha suppression. (b) Same as in (a), but for the 12 Hz SSR driven by
 422 the right stimulus in overlapping right-hemispheric parieto-occipital electrode clusters. (c,d) Similar
 423 to (a) but for attention-related gain effects on SSR ITCz (z-scored, y-axis) in (c) and gain effects on SSR
 424 evoked power in (d), both collapsed across electrode clusters showing 10- and 12-Hz SSR attention
 425 effects. Alpha suppression was collapsed across left- and right-hemispheric electrode clusters (see
 426 Figure 3).
 427

428 Finally, we repeated this analysis for attention effects on inter-trial phase coherence (ITC). Because
 429 SSR ITC attention effects did not show a clear topographical lateralisation (Figure 4), they were

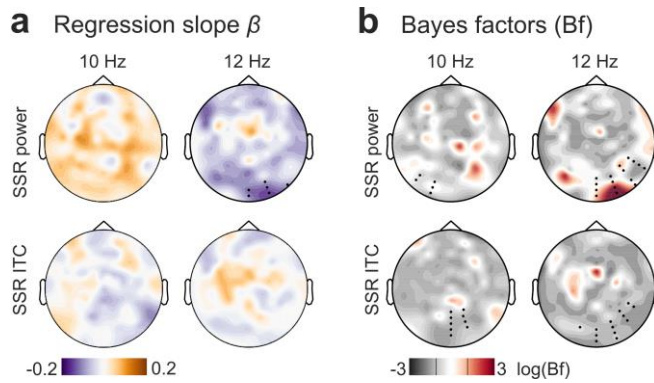
430 collapsed across driving frequencies (10 & 12 Hz). Again, findings were inconclusive when looking
431 into the correlation between these aggregate SSR ITC gain effects and a hemisphere-collapsed alpha
432 suppression index ($\tau_b = -0.059$, 95%-CrI = [-0.349 0.251]; $BF_{01} = 2.653$). Correlating collapsed attention
433 effects of SSR evoked power with the same pooled alpha suppression index yielded identical results
434 regarding the rank correlation (also see linear fits in *Figure 5*).

435 **Alpha and SSR attention effects – subject level regression**

436 A more fine-grained analysis of single-trial co-variation of alpha power lateralisation and SSR gain
437 effects during focussed spatial attention largely corroborated the group level results. Clustering
438 across EEG sensors, we found that only the 12-Hz SSR evoked power attention effect and alpha
439 lateralisation co-varied systematically across participants at occipital sites (permutation test,
440 $T_{sum} = -17.517$, $p = 0.023$). The negative sign of the slope however contradicted the expected positive
441 relationship (*Figure 6a*). Neither 10-Hz SSR evoked power nor SSR ITC (both frequencies) revealed
442 similar systematic relationships with alpha power.

443 Additionally, we used Bayesian inference on the distributions of individual regression slopes
444 (indicating the linear relationship between alpha and SSR attention effects) by sensor to quantify the
445 plausibility of either H_1 or H_0 in scalp maps (*Figure 6b*). We further overlaid these scalp maps with
446 electrode clusters showing SSR attention effects (compare with *Figure 4*). Average Bayes factors (Bfs)
447 within clusters indicated that evidence for or against any type of linear relationship remained
448 inconclusive for 10-Hz (mean $Bf_{01} = 1.422$ range = 0.639 – 2.343) and 12-Hz SSR evoked power (mean
449 $Bf_{01} = 1.245$ range = 0.153 – 3.673), although it should be mentioned that the 12-Hz cluster contained
450 a local maximum ($Bf_{10} = 1/Bf_{01} = 6.534$) that coincided topographically with the effect identified by
451 the cluster-based permutation test. For ITC evidence favoured H_0 , i.e. the absence of any relationship
452 with 10-Hz (mean $Bf_{01} = 3.040$, range = 1.861 – 4.014) and 12-Hz SSR ($Bf_{01} = 3.030$, range = 1.391 –
453 4.016) was 3 times more likely given our data.

454 Our findings show a fine distinction between SSR evoked power and ITC gain effects with respect to a
455 possible connection to alpha lateralisation in that only the latter provided conclusive evidence
456 against such a relationship. As a likely explanation, SSR evoked power still contains residual alpha
457 activity that confounds tests for covariation. Conversely, the single-trial power normalisation step
458 undertaken during the calculation of SSR ITC makes it less susceptible to this confound. Taken
459 together, the findings of this analysis do not support a positive linear relationship of alpha
460 lateralisation and SSR gain effects (especially on ITC). Therefore, it is unlikely that the counter-
461 intuitive topography of SSR attentional modulation is a reflection of alpha power lateralisation during
462 focused spatial attention.



463

464 **Figure 6** Summary of subject-level analysis of the linear relationship between alpha power and SSR
465 attentional modulation. (a) depicts the topographical distribution of group-averaged (N=17)
466 regression coefficients β (slopes) for SSR evoked power (top row) and SSR inter-trial coherence (ITC,
467 bottom row), separated by SSR frequencies 10 Hz (left column) and 12 Hz (right column). Hot colours
468 indicate a positive linear relationship and cool colours a negative relationship. Black dots in the upper
469 right panel indicate a cluster of electrodes showing a systematic effect ($p < 0.05$, cluster-based
470 permutation test) absent in tests illustrated in the other 3 panels. (b) Results of sensor-by-sensor
471 group-level Bayesian inference (Bayesian t-tests) of regression slopes against zero, plotted as
472 topographies on a $\log(BF_{10})$ scale. Plots arranged as in (a). Red colours indicate stronger evidence for
473 H_1 , grey colours indicate stronger evidence for H_0 . Black lines in the colour scale below scalp maps
474 denote thresholds that signal moderate evidence for H_0 ($\log(1/3) = -1.099$) or H_1 ($\log(3) = 1.099$) by
475 convention. Superimposed black dots indicate clusters showing systematic attention effects on SSR
476 evoked power / ITC as depicted in Figure 4 for comparison.

477

478 DISCUSSION

479 We found that two common spectral measures of alpha-band EEG during alpha-rhythmic visual
480 stimulation reflect effects of spatial attention with opposite signs. In the following we discuss how
481 this finding supports the notion of two complementary neural mechanisms governing the cortical
482 processing of dynamic visual input.

483 Analysis approach determines sign of attentional modulation

484 When focussing on the spectral representation of ongoing EEG power, we observed the prototypical
485 broad peak in the alpha frequency range (8 – 13 Hz; Figure 2). Moreover, alpha power decreased
486 over the hemisphere contralateral to the attended stimulus position, indicating a functional
487 disinhibition of cortical areas representing task-relevant regions of the visual field (Worden et al.,
488 2000; Kelly et al., 2006; Thut et al., 2006). Concurrently, alpha power increased over the ipsilateral
489 hemisphere, actively suppressing irrelevant and possibly distracting input (Rihs et al., 2007; Capilla et
490 al., 2012).

491 A second approach focussed on the SSRs, i.e. strictly stimulus-locked rhythmic EEG components. As
492 in classical frequency-tagging studies, we found spectrally distinct SSRs at the stimulation frequencies

493 (here 10 and 12 Hz). These two concurrent rhythmic brain responses thus precisely reflected the
494 temporal dynamics of the visual stimulation. Notably, SSR evoked power was between one to two
495 orders of magnitude (10 – 100 times) lower than ongoing-alpha power. Smaller evoked power also
496 explained why SSRs remained invisible in spectra of ongoing activity. They were likely masked by the
497 broad alpha peak (Figure 2; Covic et al., 2017). Note that this is a result of the relatively low-intensity
498 stimulation used here. Stimulation of higher intensity can evoke SSRs that are readily visible in power
499 spectra of ongoing activity (Gulbinaite et al., 2019).

500 Crucially, we examined SSRs for effects of focused spatial attention. Visual cortical regions
501 contralateral to the respective driving stimuli showed maximum SSR evoked power. We would
502 expect to observe a decrease in SSR evoked power with attention (Kizuk and Mathewson, 2017;
503 Gulbinaite et al., 2019) under the assumption that SSRs are frequency-specific neural signatures of a
504 local entrainment of intrinsic alpha generators (Spaak et al., 2014; Notbohm et al., 2016) and exhibit
505 similar functional characteristics. Instead, we found that SSR evoked power increased in line with
506 earlier reports (Kim et al., 2007; Kashiwase et al., 2012; Keitel et al., 2013).

507 Note however that these attentional gain effects did not coincide topographically with scalp
508 locations of maximum SSR evoked power (Figure 4). Instead, they were most pronounced over
509 hemispheres ipsilateral to the position of the respective driving stimuli and thus co-localised with
510 ipsilateral alpha power increases (Figure 3). Two control analyses showed that these effects were
511 unlikely to be related (Figure 5 & 6). We have described the apparent counter-intuitive lateralisation
512 of this effect before (Keitel et al., 2017a) when comparing scalp distributions by means of Attended-
513 minus-Unattended contrasts (Keitel et al., 2017a). In that case, expecting attention effects to emerge
514 at sites of maximum SSR power entails the implicit assumption that attention only acts as a local
515 response gain mechanism. Alternatively, neural representations of attended stimuli could access
516 higher order visual processing (Lithari et al., 2016) and a gain in spatial extent could then produce
517 seemingly ipsilateral effects when evaluating topographical differences as observed here. However,
518 previous cortical source reconstructions of SSRs in lateralised stimulus situations have unequivocally
519 localised maximum effects of visuo-spatial attention to contralateral visual cortices (Müller et al.,
520 1998b; Lauritzen et al., 2010; Keitel et al., 2013). Considering the limited spatial resolution of EEG,
521 and that SSR inter-trial phase coherence showed yet another non-lateralised topographical
522 distribution for gain effects (Figure 4), warrants a dedicated neuroimaging analysis of the underlying
523 cortical sources that generate these attentional modulations.

524 **Opposite but co-occurring attention effects suggest interplay of distinct attention-related**
525 **processes**

526 Our analysis compared attention effects between “ongoing” spectral power within the alpha
527 frequency band and a quantity termed SSR “evoked power” that is commonly used in frequency
528 tagging research (Colon et al., 2012; Porcu et al., 2013; Stormer et al., 2014; Walter et al., 2016;
529 Martinovic and Andersen, 2018). This term is somewhat misleading because it conflates a power
530 estimate with the consistency of the phase of the SSR across trials of the experiment. Inter-trial
531 phase consistency (ITC) is closely related to evoked power but involves an extra normalisation term
532 that abolishes (or at least greatly attenuates) the power contribution¹ (Cohen, 2014; Gross, 2014)
533 and has been used to quantify SSRs before (Ruhnau et al., 2016).

534 The effects of attention on SSR evoked power and ITC are typically interchangeable (Covic et al.,
535 2017; Keitel et al., 2017a). In fact, increased ITC, or phase synchronisation, has been considered the
536 primary effect of attention on stimulus-driven periodic brain responses (Kim et al., 2007; Kranczioch,
537 2017). Looking at spectral power and ITC separately, as two distinct aspects of rhythmic brain
538 activity, therefore resolves the attentional modulation conundrum: Seemingly opposing attention-
539 related effects likely index different but parallel influences on cortical processing of rhythmic visual
540 input. To avoid confusion, we therefore suggest opting for ITC (or related measures, e.g. the cosine
541 similarity index (Chou and Hsu, 2018)) instead of “evoked power” to evaluate SSRs.

542 Incorporating our findings into an account that regards SSRs primarily as stimulus-driven entrainment
543 of intrinsic alpha rhythms would require demonstrating how a decrease in alpha-band power (i.e. the
544 contralateral alpha suppression) can co-occur with increased SSR phase synchronisation.

545 Alternatively, stimulus-locked (“evoked”) and intrinsic alpha rhythms could be considered distinct
546 processes (Freunberger et al., 2009; Sauseng, 2012). Consequentially, alpha range SSRs could
547 predominantly reflect an early cortical mechanism for the tracking of fluctuations in stimulus-specific
548 visual input per se (Keitel et al., 2017a) without the need to assume entrainment (Capilla et al., 2011;
549 Keitel et al., 2014).

550 The underlying neural mechanism might similarly work for a range of rhythmic and quasi-rhythmic
551 stimuli owing to the fact that visual cortex comprises a manifold of different feature detectors that
552 closely mirror changes along the dimensions of colour, luminance, contrast, spatial frequency and
553 more (Buracas et al., 1998; Blaser et al., 2000; Martinovic and Andersen, 2018). Most importantly, for
554 (quasi-)rhythmic sensory input, attention to the driving stimulus may increase neural phase-locking
555 to the stimulus to allow for enhanced tracking of its dynamics, i.e. increased fidelity. This effect has
556 been observed for quasi-rhythmic low-frequency visual speech signals (Crosse et al., 2015; Park et al.,

557 2016; Hauswald et al., 2018) and task-irrelevant visual stimuli at attended vs ignored spatial locations
558 (Keitel et al., 2017a).

559 Concurrent retinotopic biasing of visual processing through alpha suppression and stronger neural
560 phase-locking to attended stimuli could therefore be regarded as complimentary mechanisms. Both
561 could act to facilitate the processing of behaviourally relevant visual input in parallel. In this context,
562 SSRs would constitute a special case and easy-to-quantify periodic signature of early visual cortices
563 tracking stimulus dynamics over time. Intrinsic alpha suppression instead may gate the access of
564 sensory information to superordinate visual processing stages (Jensen and Mazaheri, 2010; Zumer et
565 al., 2014) and enhanced ipsilateral alpha power may additionally attenuate irrelevant and possibly
566 distracting stimuli at ignored locations (Capilla et al., 2012).

567 A neuronal implementation may work like this: During rest or inattention, occipital neuronal
568 populations synchronise with a strong internal, thalamo-cortical pacemaker (alpha). During attentive
569 processing of sensory input, retinotopic alpha suppression releases specific neuronal sub-populations
570 from an internal reign and allows them to track the stimulus dynamics at attended locations. A
571 related mechanism has been observed in the striatum, where local field potentials are dominated by
572 synchronous oscillatory activity across large areas (Courtemanche et al., 2003). However, during task
573 performance focal neuronal populations were found to disengage from this global synchronicity in a
574 consistent and task-specific manner. At the level of EEG/MEG recordings, such a mechanism could
575 lead to task-related decrease of oscillatory power but increase of coherence or ITC, as observed in
576 the current study and previously in the sensorimotor system (Gross et al., 2005; Schoffelen et al.,
577 2005; Schoffelen et al., 2011).

578 Whereas such an account challenges the occurrence of strictly stimulus-driven alpha entrainment, it
579 may still allow alpha to exert temporally precise top-down influences during predictable and
580 behaviourally relevant rhythmic stimulation – a process that itself could be subject to entrainment
581 (Thut et al., 2011; Nobre et al., 2012; Haegens and Zion Golumbic, 2018; Zoefel et al., 2018).

582 **Conclusion**

583 Our findings reconcile seemingly contradictory findings regarding spatial attention effects on alpha-
584 rhythmic activity, assumed to be entrained by periodic visual stimulation, and SSRs. Focusing on
585 spectral power or phase consistency of the EEG during visual stimulation yielded reversed attention
586 effects in the same dataset. Our findings encourage a careful and consistent choice of measures of
587 ongoing brain dynamics (here power) or measures of stimulus-related activity (here ITC), that should
588 be critically informed by the experimental question, when studying the effects of visuo-spatial

589 selective attention on the cortical processing of dynamic (quasi-) rhythmic visual stimulation. Again,
590 we emphasise that both common data analysis approaches taken here can be equally valid and
591 legitimate, yet they likely represent distinct neural phenomena. These can occur simultaneously, as
592 in our case, and may index distinct cortical processes that work in concert to facilitate the processing
593 of visual stimulation at attended locations.

594

595 **Notes**

596 ¹ In a noisy, finite signal such as the typical second(s)-long EEG epoch, there will be a positive
597 relationship between the power and inter-trial phase consistency at any frequency as is shown by the
598 greater than zero noise floor in our ITC spectra (Figure 4). Also note that ITC only measures SSRs
599 meaningfully if the neurophysiological signal contains a periodic component at the stimulation
600 frequency.

601

602 **Competing interests**

603 The authors declare no competing interests.

604

605 **Author contributions**

606 CK designed research, performed research, analysed data and wrote the article. JG designed research
607 analysed data and wrote the article. AK, CSYB, CD and GT designed research and wrote the article.

608

609 **Data accessibility**

610 EEG data, pre-processed in Fieldtrip format, that underlie all analyses reported here and a
611 corresponding MATLAB analysis script are available on the Open Science Framework, osf.io/apsyf
612 (Keitel et al., 2017b).

613

614 **References**

615

616 Adrian ED, Matthews BH (1934) The interpretation of potential waves in the cortex. *J Physiol* 81:440-
617 471.

618 Andersen SK, Muller MM (2015) Driving steady-state visual evoked potentials at arbitrary frequencies
619 using temporal interpolation of stimulus presentation. *BMC Neurosci* 16:95.

- 620 Benwell CSY, Keitel C, Harvey M, Gross J, Thut G (2018) Trial-by-trial co-variation of pre-stimulus EEG
621 alpha power and visuospatial bias reflects a mixture of stochastic and deterministic effects.
622 Eur J Neurosci 48:2566-2584.
- 623 Benwell CSY, Tagliabue CF, Veniero D, Cecere R, Savazzi S, Thut G (2017) Prestimulus EEG Power
624 Predicts Conscious Awareness But Not Objective Visual Performance. eNeuro 4.
- 625 Blaser E, Pylyshyn ZW, Holcombe AO (2000) Tracking an object through feature space. Nature
626 408:196-199.
- 627 Bonnefond M, Jensen O (2012) Alpha oscillations serve to protect working memory maintenance
628 against anticipated distracters. Curr Biol 22:1969-1974.
- 629 Buracas GT, Zador AM, DeWeese MR, Albright TD (1998) Efficient discrimination of temporal patterns
630 by motion-sensitive neurons in primate visual cortex. Neuron 20:959-969.
- 631 Capilla A, Pazo-Alvarez P, Darriba A, Campo P, Gross J (2011) Steady-state visual evoked potentials
632 can be explained by temporal superposition of transient event-related responses. PLoS One
633 6:e14543.
- 634 Capilla A, Schoffelen J-M, Paterson G, Thut G, Gross J (2012) Dissociated α -Band Modulations in the
635 Dorsal and Ventral Visual Pathways in Visuospatial Attention and Perception. Cerebral
636 Cortex.
- 637 Chou EP, Hsu SM (2018) Cosine similarity as a sample size-free measure to quantify phase clustering
638 within a single neurophysiological signal. J Neurosci Methods 295:111-120.
- 639 Cohen MX (2014) Analyzing neural time series data: theory and practice. Cambridge, Massachusetts:
640 MIT Press.
- 641 Colon E, Nozaradan S, Legrain V, Mouraux A (2012) Steady-state evoked potentials to tag specific
642 components of nociceptive cortical processing. Neuroimage 60:571-581.
- 643 Courtemanche R, Fujii N, Graybiel AM (2003) Synchronous, focally modulated beta-band oscillations
644 characterize local field potential activity in the striatum of awake behaving monkeys.
645 Journal of Neuroscience 23:11741-11752.
- 646 Covic A, Keitel C, Porcu E, Schroger E, Muller MM (2017) Audio-visual synchrony and spatial attention
647 enhance processing of dynamic visual stimulation independently and in parallel: A
648 frequency-tagging study. Neuroimage 161:32-42.
- 649 Crosse MJ, Butler JS, Lalor EC (2015) Congruent Visual Speech Enhances Cortical Entrainment to
650 Continuous Auditory Speech in Noise-Free Conditions. J Neurosci 35:14195-14204.
- 651 Delorme A, Makeig S (2004) EEGLAB: an open source toolbox for analysis of single-trial EEG dynamics
652 including independent component analysis. J Neurosci Methods 134:9-21.

- 653 Ferree TC (2006) Spherical splines and average referencing in scalp electroencephalography. *Brain*
654 *Topogr* 19:43-52.
- 655 Freunberger R, Fellingner R, Sauseng P, Gruber W, Klimesch W (2009) Dissociation between phase-
656 locked and nonphase-locked alpha oscillations in a working memory task. *Hum Brain Mapp*
657 30:3417-3425.
- 658 Groppe DM, Bickel S, Keller CJ, Jain SK, Hwang ST, Harden C, Mehta AD (2013) Dominant frequencies
659 of resting human brain activity as measured by the electrocorticogram. *Neuroimage*
660 79:223-233.
- 661 Gross J (2014) Analytical methods and experimental approaches for electrophysiological studies of
662 brain oscillations. *J Neurosci Methods* 228:57-66.
- 663 Gross J, Pollok B, Dirks M, Timmermann L, Butz M, Schnitzler A (2005) Task-dependent oscillations
664 during unimanual and bimanual movements in the human primary motor cortex and SMA
665 studied with magnetoencephalography. *Neuroimage* 26:91-98.
- 666 Gulbinaite R, Roozendaal D, VanRullen R (2019) Attention differentially modulates the amplitude of
667 resonance frequencies in the visual cortex. *bioRxiv*.
- 668 Gulbinaite R, van Viegen T, Wieling M, Cohen MX, VanRullen R (2017) Individual Alpha Peak
669 Frequency Predicts 10 Hz Flicker Effects on Selective Attention. *J Neurosci* 37:10173-10184.
- 670 Haegens S, Zion Golumbic E (2018) Rhythmic facilitation of sensory processing: A critical review.
671 *Neurosci Biobehav Rev* 86:150-165.
- 672 Hauswald A, Lithari C, Collignon O, Leonardelli E, Weisz N (2018) A Visual Cortical Network for
673 Deriving Phonological Information from Intelligible Lip Movements. *Curr Biol* 28:1453-1459
674 e1453.
- 675 Herring JD, Thut G, Jensen O, Bergmann TO (2015) Attention Modulates TMS-Locked Alpha
676 Oscillations in the Visual Cortex. *J Neurosci* 35:14435-14447.
- 677 Herrmann CS (2001) Human EEG responses to 1-100 Hz flicker: resonance phenomena in visual
678 cortex and their potential correlation to cognitive phenomena. *Exp Brain Res* 137:346-353.
- 679 Herrmann CS, Munk MH, Engel AK (2004) Cognitive functions of gamma-band activity: memory
680 match and utilization. *Trends Cogn Sci* 8:347-355.
- 681 Iemi L, Chaumon M, Crouzet SM, Busch NA (2017) Spontaneous Neural Oscillations Bias Perception
682 by Modulating Baseline Excitability. *J Neurosci* 37:807-819.
- 683 JASP-Team (2018) JASP. In, 0.8.2 Edition.
- 684 Jensen O, Mazaheri A (2010) Shaping functional architecture by oscillatory alpha activity: gating by
685 inhibition. *Front Hum Neurosci* 4:186.

- 686 Kashiwase Y, Matsumiya K, Kuriki I, Shioiri S (2012) Time courses of attentional modulation in neural
687 amplification and synchronization measured with steady-state visual-evoked potentials. *J*
688 *Cogn Neurosci* 24:1779-1793.
- 689 Kayser J, Tenke CE (2015) On the benefits of using surface Laplacian (current source density)
690 methodology in electrophysiology. *Int J Psychophysiol* 97:171-173.
- 691 Keitel A, Gross J (2016) Individual Human Brain Areas Can Be Identified from Their Characteristic
692 Spectral Activation Fingerprints. *PLoS Biology* 14:e1002498.
- 693 Keitel C, Quigley C, Ruhnau P (2014) Stimulus-Driven Brain Oscillations in the Alpha Range:
694 Entrainment of Intrinsic Rhythms or Frequency-Following Response? *Journal of*
695 *Neuroscience* 34:10137-10140.
- 696 Keitel C, Thut G, Gross J (2017a) Visual cortex responses reflect temporal structure of continuous
697 quasi-rhythmic sensory stimulation. *Neuroimage* 146:58-70.
- 698 Keitel C, Andersen SK, Quigley C, Muller MM (2013) Independent Effects of Attentional Gain Control
699 and Competitive Interactions on Visual Stimulus Processing. *Cerebral Cortex* 23:940-946.
- 700 Keitel C, Benwell CSY, Thut G, Gross J (2017b) Alpha during quasi-periodic visual stimulation. In. *Open*
701 *Science Framework*.
- 702 Keitel C, Benwell CSY, Thut G, Gross J (2018) No changes in parieto-occipital alpha during neural
703 phase locking to visual quasi-periodic theta-, alpha-, and beta-band stimulation. *Eur J*
704 *Neurosci*.
- 705 Kelly SP, Lalor EC, Reilly RB, Foxe JJ (2006) Increases in alpha oscillatory power reflect an active
706 retinotopic mechanism for distracter suppression during sustained visuospatial attention. *J*
707 *Neurophysiol* 95:3844-3851.
- 708 Kim YJ, Grabowecy M, Paller KA, Muthu K, Suzuki S (2007) Attention induces synchronization-based
709 response gain in steady-state visual evoked potentials. *Nat Neurosci* 10:117-125.
- 710 Kizuk SA, Mathewson KE (2017) Power and Phase of Alpha Oscillations Reveal an Interaction between
711 Spatial and Temporal Visual Attention. *J Cogn Neurosci* 29:480-494.
- 712 Kranczioch C (2017) Individual differences in dual-target RSVP task performance relate to
713 entrainment but not to individual alpha frequency. *PLoS One* 12:e0178934.
- 714 Lauritzen TZ, Ales JM, Wade AR (2010) The effects of visuospatial attention measured across visual
715 cortex using source-imaged, steady-state EEG. *J Vis* 10.
- 716 Lithari C, Sanchez-Garcia C, Ruhnau P, Weisz N (2016) Large-scale network-level processes during
717 entrainment. *Brain Res* 1635:143-152.
- 718 Maris E, Oostenveld R (2007) Nonparametric statistical testing of EEG- and MEG-data. *J Neurosci*
719 *Methods* 164:177-190.

- 720 Martinovic J, Andersen SK (2018) Cortical summation and attentional modulation of combined
721 chromatic and luminance signals. *Neuroimage* 176:390-403.
- 722 Mathewson KE, Prudhomme C, Fabiani M, Beck DM, Lleras A, Gratton G (2012) Making waves in the
723 stream of consciousness: entraining oscillations in EEG alpha and fluctuations in visual
724 awareness with rhythmic visual stimulation. *J Cogn Neurosci* 24:2321-2333.
- 725 Moratti S, Clementz BA, Gao Y, Ortiz T, Keil A (2007) Neural mechanisms of evoked oscillations:
726 stability and interaction with transient events. *Hum Brain Mapp* 28:1318-1333.
- 727 Morgan ST, Hansen JC, Hillyard SA (1996) Selective attention to stimulus location modulates the
728 steady-state visual evoked potential. *Proceedings of the National Academy of Sciences of*
729 *the United States of America* 93:4770-4774.
- 730 Müller MM, Teder-Sälejärvi W, Hillyard SA (1998a) The time course of cortical facilitation during cued
731 shifts of spatial attention. *Nat Neurosci* 1:631-634.
- 732 Müller MM, Picton TW, Valdes-Sosa P, Riera J, Teder-Salejarvi WA, Hillyard SA (1998b) Effects of
733 spatial selective attention on the steady-state visual evoked potential in the 20-28 Hz range.
734 *Brain Res Cogn Brain Res* 6:249-261.
- 735 Nobre AC, Rohenkohl G, Stokes M (2012) Nervous anticipation: top-down biasing across space and
736 time. In: *Cognitive Neuroscience of Attention*, 2 Edition (Posner MI, ed), pp 159-186. New
737 York: Guilford.
- 738 Nolan H, Whelan R, Reilly RB (2010) FASTER: Fully Automated Statistical Thresholding for EEG artifact
739 Rejection. *J Neurosci Methods* 192:152-162.
- 740 Norcia AM, Appelbaum LG, Ales JM, Cottareau BR, Rossion B (2015) The steady-state visual evoked
741 potential in vision research: A review. *J Vis* 15:4.
- 742 Notbohm A, Kurths J, Herrmann CS (2016) Modification of Brain Oscillations via Rhythmic Light
743 Stimulation Provides Evidence for Entrainment but Not for Superposition of Event-Related
744 Responses. *Front Hum Neurosci* 10:10.
- 745 Oostenveld R, Praamstra P (2001) The five percent electrode system for high-resolution EEG and ERP
746 measurements. *Clin Neurophysiol* 112:713-719.
- 747 Oostenveld R, Fries P, Maris E, Schoffelen JM (2011) FieldTrip: Open source software for advanced
748 analysis of MEG, EEG, and invasive electrophysiological data. *Comput Intell Neurosci*
749 2011:156869.
- 750 Park H, Kayser C, Thut G, Gross J (2016) Lip movements entrain the observers' low-frequency brain
751 oscillations to facilitate speech intelligibility. *Elife* 5.
- 752 Perrin F, Pernier J, Bertrand O, Giard MH, Echallier JF (1987) Mapping of scalp potentials by surface
753 spline interpolation. *Electroencephalogr Clin Neurophysiol* 66:75-81.

- 754 Picton TW, John MS, Purcell DW, Plourde G (2003) Human auditory steady-state responses: the
755 effects of recording technique and state of arousal. *Anesth Analg* 97:1396-1402.
- 756 Porcu E, Keitel C, Muller MM (2013) Concurrent visual and tactile steady-state evoked potentials
757 index allocation of inter-modal attention: a frequency-tagging study. *Neurosci Lett* 556:113-
758 117.
- 759 Regan D (1966) Some characteristics of average steady-state and transient responses evoked by
760 modulated light. *Electroencephalogr Clin Neurophysiol* 20:238-248.
- 761 Richter CG, Thompson WH, Bosman CA, Fries P (2015) A jackknife approach to quantifying single-trial
762 correlation between covariance-based metrics undefined on a single-trial basis.
763 *Neuroimage* 114:57-70.
- 764 Rihs TA, Michel CM, Thut G (2007) Mechanisms of selective inhibition in visual spatial attention are
765 indexed by alpha-band EEG synchronization. *Eur J Neurosci* 25:603-610.
- 766 Rouder JN, Morey RD, Speckman PL, Province JM (2012) Default Bayes factors for ANOVA designs.
767 *Journal of Mathematical Psychology* 56:356-374.
- 768 Rouder JN, Speckman PL, Sun DC, Morey RD, Iverson G (2009) Bayesian t tests for accepting and
769 rejecting the null hypothesis. *Psychonomic Bulletin & Review* 16:225-237.
- 770 Ruhnau P, Keitel C, Lithari C, Weisz N, Neuling T (2016) Flicker-Driven Responses in Visual Cortex
771 Change during Matched-Frequency Transcranial Alternating Current Stimulation. *Front Hum*
772 *Neurosci* 10:184.
- 773 Samaha J, Iemi L, Postle BR (2017) Prestimulus alpha-band power biases visual discrimination
774 confidence, but not accuracy. *Conscious Cogn* 54:47-55.
- 775 Samaha J, Bauer P, Cimaroli S, Postle BR (2015) Top-down control of the phase of alpha-band
776 oscillations as a mechanism for temporal prediction. *Proc Natl Acad Sci U S A* 112:8439-
777 8444.
- 778 Sauseng P (2012) Brain oscillations: phase-locked EEG alpha controls perception. *Curr Biol* 22:R306-
779 308.
- 780 Schoffelen JM, Oostenveld R, Fries P (2005) Neuronal coherence as a mechanism of effective
781 corticospinal interaction. *Science* 308:111-113.
- 782 Schoffelen JM, Poort J, Oostenveld R, Fries P (2011) Selective movement preparation is subserved by
783 selective increases in corticomuscular gamma-band coherence. *J Neurosci* 31:6750-6758.
- 784 Schonbrodt FD, Wagenmakers EJ (2017) Bayes factor design analysis: Planning for compelling
785 evidence. *Psychon Bull Rev*.
- 786 Spaak E, de Lange FP, Jensen O (2014) Local entrainment of alpha oscillations by visual stimuli causes
787 cyclic modulation of perception. *J Neurosci* 34:3536-3544.

- 788 Stormer VS, Alvarez GA, Cavanagh P (2014) Within-hemifield competition in early visual areas limits
789 the ability to track multiple objects with attention. *J Neurosci* 34:11526-11533.
- 790 Tallon-Baudry C, Bertrand O, Delpuech C, Pernier J (1996) Stimulus specificity of phase-locked and
791 non-phase-locked 40 Hz visual responses in human. *J Neurosci* 16:4240-4249.
- 792 Tallon-Baudry C, Bertrand O, Peronnet F, Pernier J (1998) Induced gamma-band activity during the
793 delay of a visual short-term memory task in humans. *J Neurosci* 18:4244-4254.
- 794 Thut G, Schyns PG, Gross J (2011) Entrainment of perceptually relevant brain oscillations by non-
795 invasive rhythmic stimulation of the human brain. *Front Psychol* 2:170.
- 796 Thut G, Nietzel A, Brandt SA, Pascual-Leone A (2006) Alpha-band electroencephalographic activity
797 over occipital cortex indexes visuospatial attention bias and predicts visual target detection.
798 *J Neurosci* 26:9494-9502.
- 799 van Diepen RM, Mazaheri A (2018) The Caveats of observing Inter-Trial Phase-Coherence in Cognitive
800 Neuroscience. *Sci Rep* 8:2990.
- 801 Vialatte FB, Maurice M, Dauwels J, Cichocki A (2010) Steady-state visually evoked potentials: focus on
802 essential paradigms and future perspectives. *Prog Neurobiol* 90:418-438.
- 803 Wagenmakers EJ, Wetzels R, Borsboom D, van der Maas HL (2011) Why psychologists must change
804 the way they analyze their data: the case of psi: comment on Bem (2011). *J Pers Soc Psychol*
805 100:426-432.
- 806 Walter S, Keitel C, Muller MM (2016) Sustained Splits of Attention within versus across Visual
807 Hemifields Produce Distinct Spatial Gain Profiles. *J Cogn Neurosci* 28:111-124.
- 808 Walter WG, Dovey VJ, Shipton H (1946) Analysis of the Electrical Response of the Human Cortex to
809 Photic Stimulation. *Nature* 158:540-541.
- 810 Worden MS, Foxe JJ, Wang N, Simpson GV (2000) Anticipatory biasing of visuospatial attention
811 indexed by retinotopically specific alpha-band electroencephalography increases over
812 occipital cortex. *J Neurosci* 20:RC63.
- 813 Zauner A, Fellingner R, Gross J, Hanslmayr S, Shapiro K, Gruber W, Muller S, Klimesch W (2012) Alpha
814 entrainment is responsible for the attentional blink phenomenon. *Neuroimage* 63:674-686.
- 815 Zoefel B, Ten Oever S, Sack AT (2018) The Involvement of Endogenous Neural Oscillations in the
816 Processing of Rhythmic Input: More Than a Regular Repetition of Evoked Neural Responses.
817 *Front Neurosci* 12:95.
- 818 Zumer JM, Scheeringa R, Schoffelen JM, Norris DG, Jensen O (2014) Occipital alpha activity during
819 stimulus processing gates the information flow to object-selective cortex. *PLoS Biology*
820 12:e1001965.
- 821